Silica Encapsulation by Miniemulsion Polymerization: Distribution and Localization of the Silica Particles in Droplets and Latex Particles

ARTICLE *in* LANGMUIR · MARCH 2012

Impact Factor: 4.46 · DOI: 10.1021/la300587b · Source: PubMed

Langmuir

Article

pubs.acs.org/Langmuir

Silica Encapsulation by Miniemulsion Polymerization: Distribution and Localization of the Silica Particles in Droplets and Latex Particles

E. Bourgeat-Lami,*[,†] G. A. Farzi,[†] L. David,[‡] J.-L. Putaux,[§] and T. F. L. McKenna[†]

[†]Université de Lyon, Université Lyon 1, CPE Lyon, CNRS, UMR 5265, Laboratoire de Chimie, Catalyse, Polymères et Procédés (C2P2), LCPP Group - 43, Boulevard du 11 Novembre 1918, F-69616, Villeurbanne Cedex, France

[‡]Université de Lyon, Université Claude Bernard Lyon 1, CNRS, UMR5223, Ingénierie des Matériaux Polymères, Laboratoire IMP@Lyon1 - 15, Boulevard Latarjet, F-69622 Villeurbanne Cedex, France

[§]Centre de Recherches sur les Macromolécules Végétales (CERMAV-CNRS), BP 53, F-38041 Grenoble Cedex 9, France affiliated with Université Joseph Fourier and a member of the Institut de Chimie Moléculaire de Grenoble

Supporting Information

ABSTRACT: The impact of including hydrophobically modified silica on the morphology of miniemulsified monomer mixtures and that of the resulting polymer particles was investigated, with emphasis placed on the distribution and localization of the inorganic phase. Silica nanoparticles with diameters of 20 and 78 nm were first modified with γ-methacryloxypropyl trimethoxysilane (γ-MPS) to favor their dispersion in methyl methacrylate (MMA)/*n*-butyl acrylate (BuA) and mixtures of varying MMA to BuA weight ratios. The monomer–silica dispersions were then emulsified by ultrasonication, and the resulting silica-loaded droplets were examined using cryo-transmission electron microscopy (cryo-TEM). This represents the first time such silica-loaded nanodroplets were examined in this way. The results of the cryo-TEM show that whereas the silica particles could easily be dispersed in MMA or a mixture of MMA and BuA to produce stable dispersions, the emulsification step promotes the (re)localization of the silica at the oil–water interfaces. It was also shown that not all droplets are equal; some droplets and particles contain no silica whereas others contain many silica particles. After the subsequent polymerization step, the silica was buried inside the latex particles.

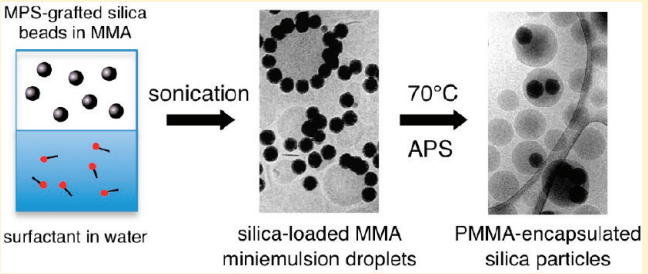

1. INTRODUCTION

The incorporation of silica particles into an organic matrix to obtain organic/inorganic hybrids via different polymerization techniques has received a great deal of attention over the past few years because of significant improvements in the mechanical and optical properties of the resulting products.[1−8] Among the different approaches to making such products, heterophase polymerization processes such as emulsion and miniemulsion polymerization are popular because they offer environmentally friendly alternatives to solvent-based systems.[9−13] Miniemulsion polymerization offers additional advantages over conventional emulsion polymerization. In particular, it is relatively easy to encapsulate hydrophobic compounds inside polymer particles by this technique because of the way in which the droplets are generated.[14−16] Indeed, unlike in conventional emulsion polymerization, miniemulsion droplets can be regarded as individually acting nanoreactors that can be converted into particles of similar size and composition. Hence, if inorganic particles are originally suspended in the monomer phase prior to polymerization, it is possible to form organic/inorganic composite particles through droplet nucleation.

A few groups have been dealing with the incorporation of silica particles into polymer latexes by this technique.[17−29] For instance, Wu and co-workers[18,19] reported on the successful synthesis of composite latex particles with various morphologies using γ-methacryloxypropyl trimethoxysilane (γ-MPS)-functionalized silica particles. A similar strategy was followed by Huang et al.[20] and by Forcada and co-workers,[21] who reported the synthesis of polymer/silica nanocomposite particles with a high silica encapsulation efficiency. Regardless of the final morphology obtained, the silica particles must be functionalized in order to render their surfaces hydrophobic and compatible with the monomer phase. The surfaces of silica particles can be modified by, for instance, the covalent attachment of polymers using chemically attached initiators for subsequently controlled radical polymerization.[28,29] Polymerizable silane coupling agents such as γ-MPS have also frequently been reported to ensure the formation of covalent bonds between the silica particles and the polymer and bring about tunable interfacial interactions.[18−22,30]

However, unlike the morphology of the functionalized particles, little attention has been paid to droplet formation in the presence of modified silica particles nor to how these droplets are transformed into polymer particles. A survey of the recent

Received: February 8, 2012
Revised: March 12, 2012
Published: March 12, 2012

   dx.doi.org/10.1021/la300587b | *Langmuir* 2012, 28, 6021−6031

literature reveals that a lot of effort has been into controlling particle morphology and that less attention has been paid to the miniemulsion polymerization mechanism itself. Indeed, until now it has been implicitly assumed that the silica particles, originally dispersed in the monomer phase, were contained inside the miniemulsion droplets after sonication. It has also been generally assumed that the final latex particles were a faithful copy of the miniemulsion droplets with a homogeneous dispersion of the functionalized silica inside them, although in practice this has rarely been the case. Indeed, several recent articles on miniemulsion encapsulation have shown the limitations of this technique, such as the small incorporation of inorganic materials, the inhomogeneous distribution of the inorganic particles, incomplete encapsulation, and the large populations of pure latex particles.[31−34]

The objective of this article is to shed more light on the mechanism of droplet formation and polymerization in silica-based miniemulsion systems. To do so, we have selected silica particles with different diameters and have carefully examined each elementary step in the process. Because efficient encapsulation requires the inorganic particles to be well-dispersed in the monomer phase,[35] particular attention was paid to finding appropriate conditions for rendering the silica particles hydrophobic and compatible with acrylic monomers. The resulting colloidal suspensions were emulsified with an aqueous solution of surfactant to form silica-loaded nanodroplets. These nanodroplets were characterized by dynamic light scattering (DLS) and cryo-transmission electron microscopy (cryo-TEM) before and after polymerization to gain insight into the mechanism of droplet formation and polymerization.

2. EXPERIMENTAL SECTION

2.1. Materials. The aqueous silica suspensions used in this study were kindly supplied by Clariant (France). The main characteristics of these suspensions (referred to as 30N12 and GEN33) are shown in Table 1. They differ by their mean particle diameters (e.g., 20 and 78 nm, respectively) and their particle size distributions, as evaluated by their polydispersity index (poly) values.

Table 1. Main Characteristics of the Silica Colloidal Suspensions Used in This Work

	30N12	GEN 33
particle diameter (D_{p,SiO_2}, nm)[a]	20	78
poly[a]	0.54	0.02
specific surface area (S_{spec}, m^2/g)[b]	254	51
solid content (SC, %)	30.5	27
suspension pH	9.9	9.6

[a]Determined by DLS. [b]Determined by BET.

γ-Methacryloxy propyl trimethoxysilane (γ-MPS, Acros Organics) was used as the coupling agent throughout this work (Scheme 1 in the Supporting Information).

Absolute ethyl alcohol (99.8%) and methyl alcohol (99.9%) were obtained from Carlo Erba and used as received. The monomers (methyl methacrylate (MMA) and butyl acrylate (BuA)), the hydrophobe (octadecylacrylate (ODA)), and the initiator (ammonium persulfate (APS)) were all obtained from Acros and used as received. Disponil A3065 (a mixture of ethoxylated linear fatty alcohols) and Disponil FES 32S (sodium lauryl ether sulfate) are nonionic (TN) and anionic (TA) surfactants that were kindly supplied by Cognis (France) as solutions of 65 and 32 wt % active matter in water, respectively. Water was deionized before use (Purelab Classic UV, Elga LabWater).

2.2. Synthesis. *2.2.1. Grafting of γ-MPS onto Silica Particles.* In a typical grafting reaction, the original aqueous silica dispersion was mixed with analytical-grade absolute ethanol up to the desired solid content (10 wt %) to ensure the colloidal stability of the silica particles. Then, a predetermined amount (15 μmol/m^2) of γ-MPS was added to the diluted silica suspension. Grafting was carried out at room temperature for 24 h under continuous stirring.[36] Finally, the sample was extensively washed with absolute ethanol via a series of centrifugation/redispersion cycles to ensure the removal of nonreacted species prior to analysis.

2.2.2. Dispersion of γ-MPS-Functionalized Silica Particles in Monomers. Organic dispersions of γ-MPS-functionalized silica in MMA/BuA mixtures of varying MMA to BuA weight ratios were prepared following the procedure reported by Ford and coworkers[37,38] and originally described by Hiltner et al.[39] Typically, the hydroalcohol suspension of γ-MPS-modified silica particles was first dialyzed against methanol and then against monomers using SpectraPor regenerated cellulose dialysis membranes (8 kDa molecular weight cutoff). The silica content in the monomer phase varied from 0 to 30% w/w. The samples were diluted in absolute ethanol prior to particle size measurements.

2.2.3. Miniemulsification of Silica-Containing Monomer Dispersions. The reaction media were ultrasonically homogenized. Preliminary experiments showed that the geometry of the sonication system and operating conditions played a key role in the miniemulsification. To ensure that the sonication step was reproducible and independent of the positioning of the probe head and the vessel geometry, a vessel of 250 mL should be charged with at least 150 g of raw material according to the formulation given in Table 2. The tip of the sonifier should be centered in the emulsification vessel. Sonication was applied at 80% amplitude of the maximum output power (Vibracell, 600 W) for 120 s while stirring with a magnetic stir bar at 500 rpm.

Table 2. Miniemulsion Recipe

water (g)	silica (g)	MMA + BuA (g)[a]	ODA (g)	surfactant (g)	APS (g)
69.35	0−8.5	28.1	2	TA, 0.17; TN, 0.26	0.12

[a]Varying MMA to BuA weight ratios: 100/0, 50/50, and 0/100.

2.2.4. Miniemulsion Polymerization. Silica/polyacrylic composite particles were prepared by polymerizing the miniemulsions according to the recipe given in Table 2. Batch polymerization was performed in a glass-jacketed reactor equipped with a condenser and a nitrogen inlet. The miniemulsion was introduced into the reactor and deoxygenated by purging with nitrogen for 20 min while the temperature was raised to 70 °C. The addition of the initiator (APS) gave the zero time of the reaction. Monomer consumption was followed by the gravimetric analysis of samples withdrawn from the polymerization medium at regular time intervals after correcting for the amount of nonvolatile products (e.g., APS, surfactant, and silica).

2.3. Characterization. The specific surface area (S_{spec}) of the silica was determined from nitrogen adsorption isotherms using the Brunauer−Emmett−Teller (BET) method.[40] Infrared spectra were recorded using a Nicolet FTIR 460 spectrometer on powder-pressed KBr pellets. ^{29}Si NMR and ^{13}C solid-state NMR were performed on a Bruker DSX-300 spectrometer operating at 59.63 and 75.47 MHz, respectively, by the use of proton cross polarization. The contact time was 5 ms, the recycle delay was 1 s, and the spinning rate was 10 kHz. The ^{29}Si and ^{13}C chemical shifts were referenced to tetramethylsilane. Carbon elemental analyses were conducted at the Service Central d'Analyze du Centre National de la Recherche Scientifique at Solaize, France using a CH elemental analyzer equipped with a CO_2/H_2O infrared detector, enabling us to determine the C content to a precision of 0.3%. The droplet and particle sizes (intensity-averaged hydrodynamic diameters, D_d and D_p, respectively) were determined by DLS using a Malvern Zetasizer HS1000. The data were collected using the fully automatic mode. The mean size distribution, poly, is a dimensionless value related to the distribution broadness determined

dx.doi.org/10.1021/la300587b | Langmuir 2012, 28, 6021−6031

from the autocorrelation function using a second-order method of cumulant analysis.[41] The number of droplets, N_d, or particles, N_p (mL^{-1}_{latex}) was calculated using the diameter obtained from dynamic light scattering (DLS) (either D_d or D_p, nm) according to eq 1, with τ being the solid content of the dispersed phase (comprising the silica, the monomer, and the polymer present for a given conversion and expressed in $g{\cdot}mL^{-1}_{latex}$) and ρ ($g{\cdot}cm^{-3}$) being the density of the particles (taking into account the amount of silica and polymer).

$$N_p,\ N_d \frac{6\tau}{\rho\pi\,(\text{diameter})^3} \times 10^{21} \quad (1)$$

In addition, the particle size and size distribution in acrylic silica suspensions were determined by small-angle X-ray scattering (SAXS) at 25 °C. The experiments were carried out at the European Synchrotron Radiation Facility (ESRF) synchrotron source in Grenoble, France on the BM02 (D2AM) beam line. The X-ray wavelength was fixed at 0.7749 Å, and the sample-to-detector distance was about 1.50 m. The SAXS data were recorded using a CCD detector (Ropper Scientific). Image processing consisted of (i) the subtraction of the image obtained with no incident beam (dark image); (ii) normalization with the transmitted intensity; (iii) normalization with the image obtained with homogeneous illumination of the camera (flat field); (iv) the correction of distortion induced by the camera; (v) radical averaging around the center of the image; and (vi) subtraction of the radial average from the corrected image obtained without a sample (in an empty cell).

Viscosity measurements were performed using an RDA III rheometer from RHEO Service using parallel plate geometry. Frequency sweeps (0.3−120 $rad{\cdot}s^{-1}$) with an applied strain of 5−10% were made on 500-μm-thick samples of 8 mm diameter at room temperature.

Gas chromatography (GC) analyses were conducted using a Hewlett-Packard HP-5890 series II instrument equipped with a flame ionization detector and a fused silica capillary column. The oven temperature was increased from 25 to 600 °C with a 10 $°C{\cdot}min^{-1}$ heating ramp.

Direct observation of the miniemulsions and latexes was carried out by cryo-TEM. As described in detail elsewhere,[42] thin liquid films of the suspensions were formed on Pelco NetMesh lacy carbon grids and vitrified by quench freezing into liquefied ethane. The grids were then mounted in a precooled Gatan 626 specimen holder, transferred to a Philips CM200 cryomicroscope operating at 80 kV, and observed at low temperature (−180 °C) under low-dose conditions. Kodak SO163 images were recorded.

3. RESULTS AND DISCUSSION

3.1. Surface Modification of Silica Particles. Qualitative evidence of γ-MPS grafting on the silica surface was provided by FTIR and solid-state NMR spectroscopy (Figures S1−S3 in the Supporting Information). It is now well accepted[43−46] that when the reaction occurs in a polar medium such as a mixture of ethanol and water, the organosilane molecules first hydrolyze. The resulting silanol groups then form hydrogen bonds with neighboring hydrolyzed silane molecules and with surface silanol groups and undergo condensation reactions with the release of water or alcohol molecules. To gain insight into the grafting process, the number of silane molecules chemically bonded to the surfaces of the silica particles was determined by elemental analysis from the difference in carbon content (ΔC, wt %) before and after grafting using the following equation[47]

$$\text{grafting density } (\mu\text{mol/m}^2) = 10^6 \times \Delta C \times [1200N_C - \Delta C(M-1)] \times S_{spec} \quad (2)$$

where N_c and M are the number of carbon atoms and the molecular weight of the grafted molecule, respectively, and S_{spec} is the specific surface area of silica determined before grafting. The grafting density of γ-MPS on the surface of the silica particles is reported in Table 3. The grafting density of γ-MPS is relatively high and of the same order of magnitude as the values reported in the literature under similar conditions.[18] The data obtained are consistent with the formation of a multilayer polyorganosiloxane coating and suggest that the grafting reaction is efficient. It is also noticeable that the grafting density is higher for the GEN33 than for the 30N12 silica particles. This is likely due to differences in particle size as previously reported in the literature.[48]

Table 3. γ-MPS Grafting Density on the Surfaces of Various Silica Particles

	30N12	GEN33
D_{pSiO_2} (nm)[a]	20	78
ΔC (%)[b]	4.2	1.9
grafting density (μmol/m^2)[c]	2.2	4.7

[a]Determined by DLS. [b]Difference in carbon content before and after grafting as determined by carbon elemental analysis. [c]Determined using eq 2.

3.2. Dispersion of the γ-MPS-Grafted Silica Particles in Monomers. If the particles are not modified well enough, then they will most likely form aggregates in the monomer phase. This is, of course, undesirable because, as previously mentioned, our ultimate goal is to obtain stable silica dispersions in monomers. The silica particle sizes and poly values were taken as indicators of colloidal stability; if the silica particle size increased during the process, then this meant that some aggregates had formed. Such aggregation in the monomer is detrimental because it would pose a problem with obtaining an acceptable droplet size distribution after miniemulsification as well as limiting the prospect of the homogeneous dispersion of the silica. The silica particle diameter (D_{SiO_2}), the poly value, and the solid content (SC) were therefore monitored after grafting and after each dialysis step. The results are shown in Table 4. The samples treated with γ-MPS did not show any significant change in particle size after grafting, dialysis in methanol, and dialysis in MMA. Moreover, no sedimentation was observed, suggesting that the γ-MPS-grafted silica particles were perfectly stable in these different media. We confirmed by GC the absence of residual methanol in the final MMA suspensions. In contrast, silica particles that were not functionalized tended to agglomerate after dialysis in MMA, as attested to by the significant increase in the diameter and in the poly value. These results showed that γ-MPS grafting onto the silica particles played a determinant role in ensuring particle

Table 4. Effect of Grafting on the Characteristics of the Silica Dispersions after Each Dialysis Step

		D_{pSiO_2} (nm)	poly	SC (%)
raw silica	after dilution in water	78	0.02	10.0
	after dialysis in methanol	75	0.07	10.4
	after dialysis in MMA	1450	0.95	13.0
γ-MPS-grafted silica	after grafting in ethanol and water	75	0.07	11.2
	after dialysis in methanol	78	0.05	11.0
	after dialysis in MMA	77	0.03	21.0

dx.doi.org/10.1021/la300587b | Langmuir 2012, 28, 6021−6031

dispersion in this particular monomer by promoting the steric stability of the colloidal silica particles. Thus, when the particles were transferred from a primarily aqueous environment to a primarily hydrophobic environment, this additional steric stabilization helped to overcome particle aggregation.

These preliminary results lead us to believe that it is possible to make the silica particles compatible with an MMA environment by grafting γ-MPS onto their surfaces. In addition, it appears that the intermediate dialysis step in methanol has a significant effect on the quality and stability of the silica suspensions. Hence, the effect of the intermediate dialysis was studied in a series of runs in which the γ-MPS-grafted silica suspensions were either dialyzed directly against MMA or dialyzed once or twice against methanol as a transition medium and then against MMA. At least one dialysis in methanol as a transition medium was necessary to obtain a stable suspension of silica in this monomer. We suggest that the solvation of the grafted poly(γ-MPS) chains on the silica surface by methanol helps the polysiloxane chains to expand in the surrounding medium and consequently provides the required steric stabilization to the silica colloid. Moreover, the fact that electrostatic repulsive forces also stabilize the particles cannot be excluded. Indeed, it is known that inorganic particles dispersed in methanol still exhibit a zeta potential because of the strong polarity of this medium.[37,38,49] When the suspension of γ-MPS-grafted silica particles is dialyzed against MMA, the methanol molecules are gradually replaced by MMA and the electrosteric stabilization becomes progressively more steric.

3.2.1. Role of the Nature of the Monomer in the Stability of the Silica Dispersions. The feasibility of dispersing silica particles in a 50/50 w/w MMA/BuA monomer mixture and in pure BuA was examined, and the results were compared to those obtained with pure MMA. Three series of colloidal silicas (GEN33) were diluted to 10% with absolute ethanol, reacted with γ-MPS, and dialyzed twice against methanol. One series of samples was further dialyzed three times against MMA and considered to be a reference sample, whereas the two other series of samples were dialyzed either against a mixture of MMA and BuA or against pure BuA. The results shown in Table 5 reveal that it is possible to disperse the surface-modified silica particles satisfactorily in both MMA and in a 50/50 MMA/BuA mixture without aggregation, as attested to by the small particle size and the relatively narrow particle size distribution. However, for pure BuA, we observed some limited sedimentation. Although the silica particle diameter remained almost constant for MMA and MMA/BuA, it dramatically increased in the case of pure BuA. Obviously, this suggests that the γ-MPS-grafted silica particles are not fully compatible with BuA. This could be explained by the nature of the coupling agent that contains residual hydroxyl groups (that have not been consumed during grafting or that have been introduced during the functionalization reaction) and is consequently more polar than BuA. It is worth noting here that unlike the case of BuA neither the MMA nor the MMA/BuA silica suspensions showed any significant variation in particle size for several days (Supporting Information, Figure S4).

Table 5. Influence of the Nature of the Monomer on the Characteristics of the γ-MPS-Grafted Silica (GEN33)−Monomer Dispersions

monomer	D_{PSiO_2} (nm)	poly	SC (%)
MMA	77	0.03	21
MMA/BuA (50/50 w/w)	81	0.05	23.5
BuA	>1000 nm	1.00	31.5

3.2.2. Influence of the Silica Weight Fraction. Dispersions of different silica fractions in monomers were prepared using the GEN33 colloidal silica suspension, which was first diluted in ethanol to prepare silica dispersions with 10, 15, 20 and 28 wt % solids. These hydroalcoholic dispersions were next reacted with the desired amount of γ-MPS, and the procedure was continued with two dialyses in methanol and three dialyses against either MMA or MMA/BuA. The samples were characterized at the end of each step. The results are summarized in Table 6. When the initial silica content was higher than 15%, the particle size increased significantly after grafting with γ-MPS, suggesting that aggregates were formed. At silica weight fractions above 28%, precipitation occurred after grafting and after dialysis in methanol. After dialysis in the monomers, we observed a further increase in the average silica particle diameter and a broadening of the particle size distribution with increasing silica content of the original suspension. The effect was more pronounced for MMA/BuA than for pure MMA. In addition, the silica particle concentration in the monomer phase was systematically higher than the initial solids content after dilution in ethanol. The concentration of silica particles increased slightly when they were transferred from pure water to methanol. However, when the samples were dialyzed in monomer, the solids content increased significantly. This might be due to the increase in the molar volume when moving from water and ethanol to methanol and then to MMA and MMA/BuA. Because the silica particles did not pass through the membrane, the concentration of silica particles increased when the molar volume of the dialysis solution increased.

We have shown that it was possible to prepare stable silica−monomer dispersions with high silica contents in both MMA (up to 22%) and MMA/BuA (50/50) (up to 35%) starting from a silica suspension that was 15% solids in ethanol. This last value was selected to continue the investigation on the 30N12 silica particles, and the results will be shown in the following paragraph for the case of an MMA/BuA mixture. The reason for this choice was that aggregates formed more easily in the mixture than in MMA alone. Hence, if it is possible to produce silica monomer dispersions in the mixture, then it will certainly be possible to do the same for pure MMA.

3.2.3. Dispersion of the 20 nm Silica Particles in a 50/50 MMA/BuA Mixture. As previously described for GEN33, the 20 nm 30N12 silica particles were functionalized by γ-MPS grafting onto their surface. The grafting was first carried out in ethanol as discussed above. Unfortunately, the suspension became destabilized upon the addition of γ-MPS. We thus decided to dilute the original silica dispersion in methanol to provide better colloidal stability to the system. After being grafted, the samples were dialyzed first against methanol and then against the monomer mixture as previously described. The samples were characterized at the end of every step, and the results are summarized in Table 7. Acceptable results were obtained when the primary silica suspension was diluted in methanol down to a 15% solids content. Under such conditions, no sedimentation was observed and relatively stable silica−monomer dispersions were obtained. The silica particle mean diameter in MMA/BuA (50/50) was found to be 33 nm by DLS, which is slightly higher than before grafting, and the poly value and solids content were 0.43 and 20.7%, respectively. We suggest that the behavior of the 30N12 silica particles is

dx.doi.org/10.1021/la300587b | Langmuir 2012, 28, 6021−6031

Table 6. Influence of the Initial Silica Concentration in Ethanol on the Characteristics of the γ-MPS-Grafted GEN33 Silica Dispersions

initial solid content in EtOH (%)	after grafting with γ-MPS	after dialysis in MeOH	after dialysis in MMA	after dialysis in MMA/BuA (50/50)
10	D_{PSiO_2} = 75 nm	D_{PSiO_2} = 77 nm	D_{PSiO_2} = 77.6 nm	D_{PSiO_2} = 81 nm
	poly = 0.07	poly = 0.03	poly = 0.03	poly = 0.05
	SC = 11.2%	SC = 11%	SC = 21%	SC = 27%
15	D_{PSiO_2} = 74 nm	D_{PSiO_2} = 82 nm	D_{PSiO_2} = 82 nm	D_{PSiO_2} = 86 nm
	poly = 0.02	poly = 0.03	poly = 0.04	poly = 0.08
	SC = 16.5%	SC = 16.1%	SC = 22%	SC = 35.1%
20	D_{PSiO_2} = 103 nm	D_{PSiO_2} = 87 nm	D_{PSiO_2} = 106 nm	D_{PSiO_2} = 161 nm
	poly = 0.3	poly = 0.04	poly = 0.14	poly = 0.1
	SC = 21.2%	SC = 21.1%	SC = 38.3%	SC = 68.3%
28	D_{PSiO_2} = /	two phases	D_{PSiO_2} = 756 nm	two phases
	poly = 1		poly = 1	
	SC = 26%		SC = 61%	

Table 7. Influence of the Diluent on the Characteristics of the γ-MPS-Grafted 30N12 Silica Dispersions

diluent	after γ-MPS grafting	after dialysis in MeOH	after dialysis in MMA/BuA (50/50)
EtOH SC = 15%	D_{PSiO_2} = 47 640 nm	sedimentation SC = 19.5%	
	poly = 0.93		
	SC = 15%		
MeOH SC = 15%	D_{PSiO_2} = 750 nm	D_{PSiO_2} = 56.4 nm	D_{PSiO_2} = 33 nm
	poly = 0.62	poly = 0.44	poly = 0.43
	SC = 15%	SC = 16.9%	SC = 20.7%

different than that of GEN33 because of their higher specific surface area. Because the amount of bound MPS is greater than the amount needed to form a monolayer in both cases, we believe that the 30N12 silica particles have a greater tendency to aggregate than do the GEN33 silica particles because they are more numerous at a given phase ratio. This might explain why some instability was seen for this product under conditions where they were not observed with the other type of silica. Nevertheless, the procedure led to relatively stable dispersions of silica particles in MMA/BuA when methanol was used as the diluent. Because methanol is more polar than ethanol, this provided the suitable hydrophilic/hydrophobic balance to maintain the colloidal stability of the suspension.

3.2.4. Characterization of the Silica/Monomer Dispersions by SAXS. Further investigation of the silica particle size and size distribution after grafting and redispersion in MMA/BuA (50/50) was performed by SAXS at 25 °C for the two silica samples and two different concentrations of 5 and 20 wt %. A detailed description of the method and modeling of the obtained data is provided in the Supporting Information. GEN33 silica dispersions exhibited a scattering pattern with characteristic oscillations at large q values comparable to that of a collection of monodisperse spheres (Figure S5b).[50] Improved modeling was obtained, accounting for an extremely narrow size distribution, by using the Pearson type VII distribution function.[51] The resulting modal value R_m was close to 37.5 nm and w was ~3.7 nm, yielding a volume-averaged mean external diameter of close to 81.5 nm, in good agreement with DLS (Table 8). In the case of the 30N12 silica suspensions, the Guinier's law predictions for an ideal dispersion[50] were clearly not appropriate because of the size distribution effects. A better modeling of such results was possible and accounted for the distribution of the radii of gyration using a Shultz number distribution function[52] (details in the Supporting Information). A rather large distribution was necessary for the modeling of the results, yielding a volume-averaged mean radius of gyration value of close to 7.0 nm (ca. a mean external diameter of $D \approx 2R_g(^5/_3)^{1/2}$, which is close to 18 nm. As seen in Table 8, this value is smaller than the DLS particle size possibly because of a few silica particles aggregates in the monomer medium. Indeed, the average diameter obtained by DLS is impacted by larger-scale nano-objects that may escape from the SAXS window. Meanwhile, SAXS analyses showed limited aggregation because the result obtained (18nm) is close to the average diameter of the untreated silica obtained by DLS (20 nm; see Table 8). These two model suspensions were used as the monomer phase in the rest of the study.

Table 8. Particle Size of Untreated and γ-MPS-Grafted Silica in Water and 50/50 MMA/BuA as Determined by DLS and SAXS

	untreated silica (water)		γ-MPS-grafted silica (MMA/BuA 50/50)		
	DLS (nm)	poly	DLS (nm)	poly	SAXS (nm)
GEN33	78	0.02	80	0.03	81.5
30N12	20	0.54	33	0.43	18

3.3. Miniemulsification of the Silica-Containing Monomer Dispersions. *3.3.1. Effect of the Silica Content on the Droplet Size.* To explore the impact of the silica content on the size of the unpolymerized droplets, different stock dispersions of silica in MMA/BuA (50/50 w/w) were prepared as described above using 20 wt % 30N12 silica (with respect to monomer) and 35 wt % GEN33. These solutions were then diluted with the appropriate amount of monomer to adjust the silica content to the desired level prior to emulsification,

dx.doi.org/10.1021/la300587b | Langmuir 2012, 28, 6021−6031

following the procedure described in the Experimental Section. It was found that the reference conditions allowed us reproducibly to generate a stable miniemulsion with droplets of about 135 nm in diameter and a poly value of close to 0.1 in the absence of silica. However, as shown in Figure 1, the

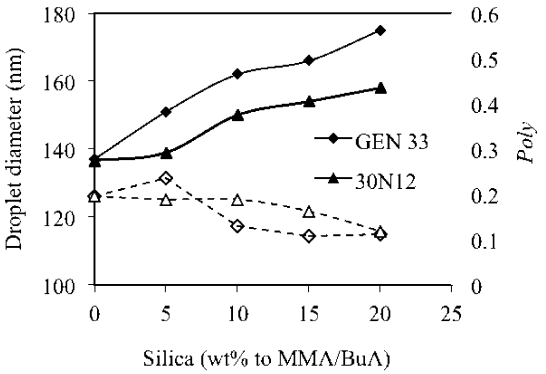

Figure 1. Average diameter (—) and poly value (---) of the miniemulsion droplets as a function of the silica content for the 30N12 (20 nm) and GEN33 (78 nm) silica particles.

presence of silica in the monomer phase has a strong influence on the droplet size and size distribution (and therefore on the droplet-formation step). The average droplet size increased significantly with increasing silica content for both the 20 and 78 nm silica particles. However, the polydispersity of the miniemulsions remained fairly constant and even decreased slightly as the silica content rose. In addition, the droplet size depended on the nature of the silica particles and is larger for the GEN33 than for the 30N12 silica. Similar behavior has been reported in the literature for both silica particles[20] and titanium dioxide (TiO_2) pigments.[53,54] In the case of TiO_2, the increase in the droplet size was attributed to the lower surfactant adsorption on the surfaces of the droplets due to the presence of the pigment. However, to the best of our knowledge, this topic has never been investigated and discussed in depth for silica particles.

Several factors might contribute to the droplet size increase when the silica content in the monomer phase increases. First, at a fixed monomer content, the presence of silica particles inside the monomer droplets may increase the volume of the droplets, consequently leading to larger droplets. However, if we assume a silica density of 1.9 g·cm^{-3}, then the change in volume of the monomer plus silica mixture will be only 13%. This would correspond to an increase in particle diameter from 137 to 143 nm. Clearly, this is not sufficient to explain the results in Figure 1. Also, because the silica particles might still be somewhat amphiphilic even after modification, they might be found at the droplet/water interface. Although it is possible that this might influence the area per surfactant molecule on the surface of the droplets, it is unlikely that this would lead to an increase in droplet size because any silica particles at the interface would act as Pickering-like surfactants that would enhance the droplet stability.[55,56]

The presence of silica particles in the monomer phase causes an increase in the viscosity of the dispersed phase. It is possible that this would make it more likely to obtain larger droplets as the viscosity increases for a fixed emulsification power input. It has been reported in the literature that the viscosity of the dispersed phase influences the droplet size in oil/water miniemulsions.[20] Mabille et al.[57] proposed a relationship between the droplet size and the ratio, R, of the viscosity of the dispersed phase to that of the continuous phase. They showed that the droplet size directly depends on the viscosity ratio to the power of 0.2.

To verify this hypothesis, the viscosity of the monomer plus silica phase was measured for different concentrations of silica particles, and the results are shown in Figure 2. As can be seen,

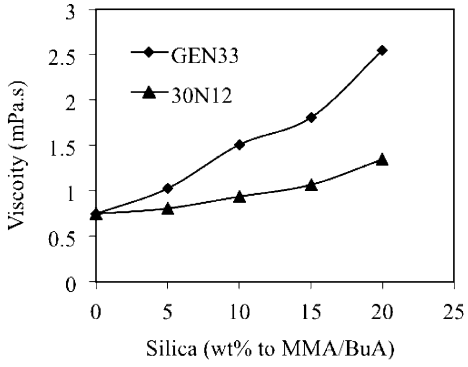

Figure 2. Variation of the viscosity of the dispersed phase as a function of the nature and concentration of the silica particles in a 50/50 w/w MMA/BuA mixture.

the viscosity of the silica/monomer dispersion increases with increasing silica content, and this effect is more important for the GEN33 than for the 30N12 silica particles. These observations are coherent with the results in Figure 1.

In fact, when the droplet diameter is plotted as a function of $R = \mu_d/\mu_c$, the curves collapse on top of each other as shown in Figure 3. The relationship between the two sets of data was

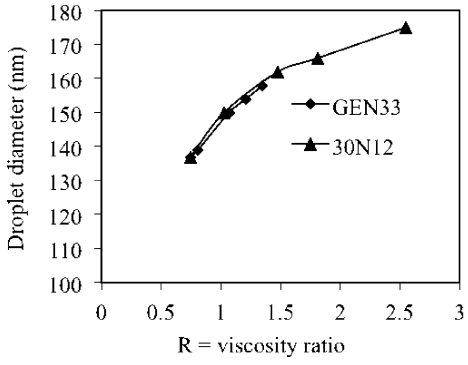

Figure 3. Relationship between the droplet size and viscosity ratio for GEN33 and 30N12 silica-loaded MMA/BuA miniemulsions.

found to follow eq 9, where the 0.22 exponent is very close to the value of 0.2 proposed by Mabille et al.:[57]

$$D_{\text{droplets}} = 147 \times R^{0.22} \quad (9)$$

It therefore appears that the change in viscosity of the dispersed phase, caused by an increase in the silica loading, appears to contribute significantly to the increase in droplet size in the present system.

3.3.2. Morphology of the Silica-Loaded Miniemulsion Droplets. Although electron microscopy is well suited to the study of the morphology of hybrid nanoparticles, problems arise when the colloidal particles are soft/liquid at room temperature and deform/flow when the suspensions are air dried on a carbon-coated TEM grid. Thus, the shape and size

dx.doi.org/10.1021/la300587b | Langmuir 2012, 28, 6021−6031

distribution cannot be accurately determined. Various methods have been reported in the literature to fix the morphology of the monomer miniemulsion prior to TEM observation such as chemical hardening and staining with osmium tetroxide[58] or freeze–fracture and replication.[59] However, these techniques all alter the morphology of the droplets to a certain extent. For what we believe to be the first time, we have observed quench-frozen silica-loaded miniemulsions embedded in vitreous ice using cryo-TEM. The images shown in Figure 4 correspond to

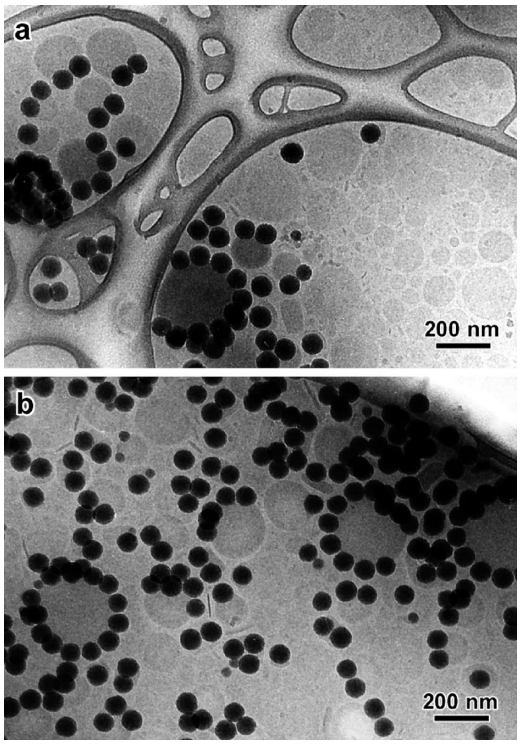

Figure 4. Cryo-TEM images of a 50/50 MMA/BuA miniemulsion containing 10 wt % GEN33 silica particles.

50/50 MMA/BuA miniemulsion droplets containing 10 wt % GEN33 silica particles. When low-dose procedures were used to prevent any significant radiation damage to the regions of interest prior to image recording, the images showed dark spherical silica particles surrounding monomer droplets that appear as gray disks. Figure 4 shows that the dispersion contains monomer droplets without silica beads as well as larger droplets with many silica beads. The monomer droplets are polydisperse, with an apparent diameter ranging from 20 to 250 nm. However, if we assume that the thickness of the embedding ice film is typically around 100–150 nm, then the monomer droplets, which are liquid prior to vitrification, were deformed by the strong confining effect of surface tension in the liquid film. Consequently, we considered that only the diameter of droplets smaller than 100 nm was reliable. The larger droplets likely adopted a lenticular shape, so their apparent diameter in the image increased. The confining effect had another consequence: the silica beads migrated to the surface of the monomer droplets. In particular, for the larger particles, the beads redistributed within the plane of the thin liquid film and formed rings around the monomer droplets.

It can also be seen in Figure 4 that despite the inhomogeneity in terms of the number of silica particles per droplet, all of the silica particles are associated with monomer droplets and appear to be located at the monomer–water interface inside the droplets. We can thus conclude that the modification with γ-MPS was successful enough that the silica could remain in the oil phase without aggregating under certain conditions. However, when the dispersion was attempted in BuA-rich mixtures, aggregates were observed. It can be concluded that we did not succeed in rendering the silica surface completely apolar with the method described above. Clearly, the silica particles have retained a certain degree of compatibility with the water phase (at least with respect to the monomer) because they all remain in the oil phase but are all essentially located at the oil–water interface.

It is also worthwhile to note that the population of silica-free monomer droplets is, on the whole, much smaller than that containing silica. It is possible that given the lower viscosity of the silica-free droplets (regardless of how they might form), they rupture more easily than do the droplets containing silica.

By analogy to Pickering emulsions, which are characterized by oil droplets surrounded by inorganic particles,[60] in the initial silica–monomer dispersions the silica beads are most likely randomly distributed on the surfaces of the monomer droplets. The fact that, in the cryo-TEM images, they often appear to form a ring around the larger monomer droplets is likely due to their migration on the surface when the monomer droplet is deformed by confinement in the thin liquid film prior to vitrification.

The variation in the number of silica beads per monomer droplet and, in particular, the presence of silica-free monomer droplets may be explained by the fact that the viscosity of the dispersed phase has a significant impact on droplet formation and droplet size. When the silica-containing monomer dispersion and the surfactant water solution are mixed together, it is to be expected that relatively large droplets (on the order of micrometers) are formed initially. According to the cryo-TEM images shown above, it is likely that the silica particles will migrate to the surface of these large droplets because of their "amphiphilic" nature. These droplets will then be fragmented into smaller ones during sonication. We propose that areas with a lower concentration of silica can be more easily fragmented than surfaces that are more densely covered with silica beads. This would create a difference in composition between the large and small droplets as schematically represented in Scheme 1.

Scheme 1. Droplet Formation and Fragmentation during Sonication[a]

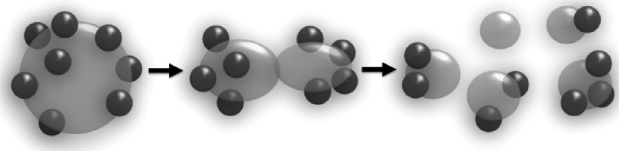

[a]The gray spheres correspond to monomer droplets whereas the black spheres are silica beads.

In conclusion, one can say that several parameters may contribute to increase the droplet size with increasing silica content. Among them, the viscosity of the dispersed phase clearly plays an important role. However, it also appears that the silica particles are not evenly distributed among the droplets and that their localization at the monomer/water interface influences the composition and size of the final droplets.

dx.doi.org/10.1021/la300587b | *Langmuir* 2012, 28, 6021–6031

3.4. Polymerization of the Silica-Loaded Miniemulsion Droplets. Figure 5 shows the evolution of conversion as a function of time and GEN33 silica content for a series of MMA/BuA (50/50) miniemulsion polymerization.

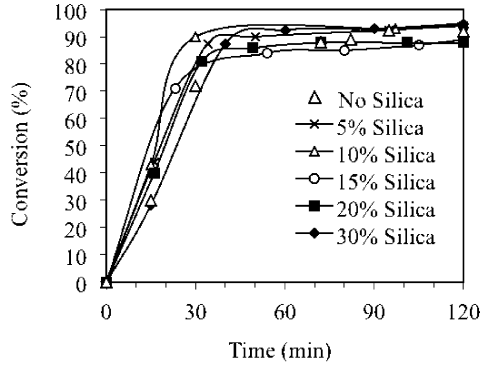

Figure 5. Conversion as a function of time for increasing concentrations of the γ-MPS-grafted GEN33 silica particles in MMA/BuA (50/50).

The conversion and rate do not appear to be strongly influenced by the silica content. One might expect to observe slightly lower polymerization rates for higher silica contents because of the larger droplet size. However, it is possible that the γ-MPS-grafted silica particles located at the monomer droplet/water interface promote the capture of oligoradicals and therefore increase the polymerization rate in the larger droplets.[13] Because these two phenomena have opposite effects, the polymerization rate is consequently not strongly influenced by the presence of silica particles. The evolution of the polymer particle size as a function of time is shown in Figure 6. The average particle size decreases at the beginning of the reaction and then increases until it reaches nearly the same size as the droplets for the samples containing less than 20 wt % silica particles. Similar experimental curves were reported by Forcada et al.[21] during the polymerization of silica-containing miniemulsion droplets. The decrease in particle size can be attributed to the generation of smaller particles at the beginning of polymerization by secondary nucleation. Because there is not enough surfactant to stabilize the newly created surface, these small particles coagulate to make larger objects.[61] For samples containing higher silica contents (typically more than 20 wt %), the droplets are larger; therefore, relatively more free surfactant is available in the aqueous phase to stabilize the newly formed particles. The average particle size thus continuously decreased throughout the polymerization. Nevertheless, the ratio of the number of particles to the number of droplets varies from 1 to a maximum of 1.6 during the reaction, before finishing at a value of close to 1 for the final product (Figure 7).

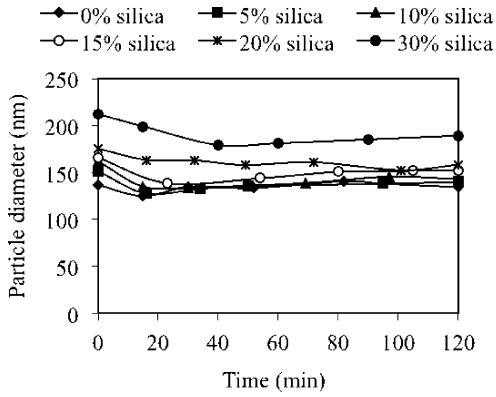

Figure 6. Particle size as a function of time for a series of MMA/BuA (50/50) miniemulsion polymerizations with increasing concentrations of the γ-MPS-grafted GEN33 silica particles.

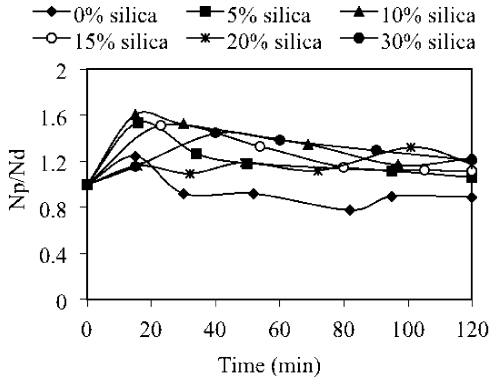

Figure 7. Evolution of N_p/N_d as a function of time for a series of MMA/BuA (50/50) miniemulsion polymerizations with increasing concentrations of γ-MPS-grafted GEN33 silica particles.

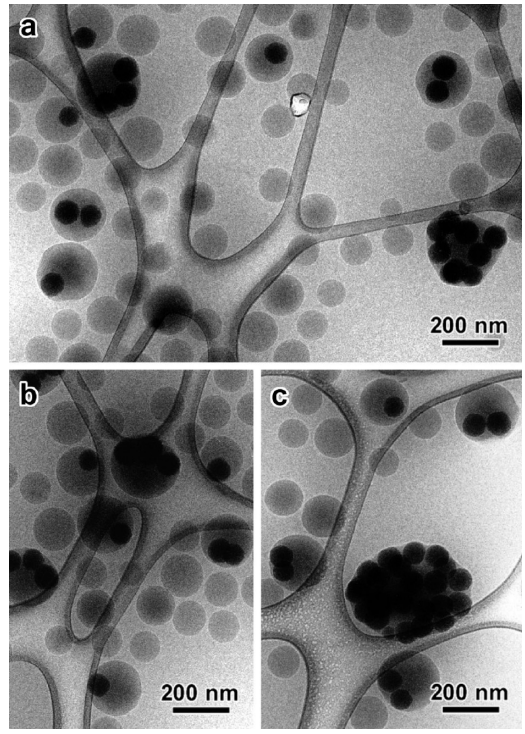

Figure 8. Cryo-TEM images of GEN33 silica/P(MMA-*co*-BuA) nanocomposite latexes with (a) 3.5 and (b, c) 20 wt % silica contents.

Figure 8 shows cryo-TEM images of P(MMA-*co*-BuA) latexes containing 3.5 and 20 wt % GEN33 silica relative to the monomer mass. The particle size ranges from 100 to 200 nm, in agreement with DLS measurements (D_p = 160 nm for 20 wt % silica). The first important point to see here is that all of the silica beads are encapsulated in polymer particles; none are found outside the particles. Large particles containing many silica beads are also occasionally seen. These particles, whose diameters are greater than 200 nm, likely originate from

dx.doi.org/10.1021/la300587b | *Langmuir* 2012, 28, 6021−6031

the polymerization of the large droplets shown in Figure 4. In polymer particles with only one silica bead, the silica appears to be ex-centered. Wu and co-workers reported similar asymmetric morphologies.[18] As can be seen in Figure 8, the silica-containing latex particles are at least 40 nm in diameter larger than those without silica, and this again appears to be similar to what we saw in Figure 4. As discussed above, the size of the miniemulsion droplet is strongly influenced by the presence of silica, and so logically is the resulting polymer particle size.

As we saw above, the silica particles were located at the interface between the monomer droplets and water. Cryo-TEM observation of the composite polymer particles revealed that the silica beads were completely embedded inside the polymer particle, sometimes just below the surface, but very rarely cleanly situated on the water interface as was the case for the droplets. This can be explained by the fact that γ-MPS, which is grafted to the silica particles, can copolymerize when free radicals are available.[36,62] Propagation of the polymer chains at the silica surface enables the inorganic particles to be gradually covered with a layer of polymer, which forms the shell of the silica/polyacrylate composite particles during the reaction step, consequently burying the particles.[13]

4. CONCLUSIONS

The grafting of γ-MPS to the silica surface renders the inorganic particles compatible enough with MMA or 50/50 MMA/BuA mixtures that loadings of solids on the order of 20 to 35 wt % could be successfully obtained depending on the size of the silica particles and the nature of the monomer phase. Interestingly enough, it was not possible to incorporate the γ-MPS-grafted silica particles into pure BuA at any level of solid content. This indicates that whereas we can stabilize the silica particles for dispersion in some mixtures, they are not totally "immune" to their immediate environment. It therefore appears that whereas the modification of silica with γ-MPS is an effective technique for the creation of polymerizable dispersions of monomer and silica, it is not sufficient to render the silica totally hydrophobic because this type of surface modification cannot be used to create silicas that are dispersible in apolar monomers such as butyl acrylate (or mixtures of monomers rich in butyl acrylate). Cryo-TEM studies of the intermediate dispersions showed that the distribution of the silica particles in the monomer droplets was heterogeneous, with some droplets containing one to several silica particles, whereas others were empty. Furthermore, the silica particles that were modified for easy dispersion in the monomer mixtures are essentially all located at the oil–water interface in the droplets. The creation of a large interface seems to promote silica migration through the monomer to the water, which is further proof that the particles have not been rendered completely hydrophobic by treatment with γ-MPS. These miniemulsions were successfully polymerized to obtain stable dispersions containing surface-modified silica particles. Further cryo-TEM studies also revealed that this inhomogeneity in the distribution of the silica beads is very similar in the final particles as well. It also showed that the silica particles appear to be covered with a layer of polymer, most likely formed by polymerization with γ-MPS.

■ ASSOCIATED CONTENT

Supporting Information

Chemical structure of γ-MPS. Characterization of silane grafting on the silica surface. Colloidal stability and SAXS analysis of the silica/monomer dispersions. This material is available free of charge via the Internet at http://pubs.acs.org.

■ AUTHOR INFORMATION

Corresponding Author

*E-mail: bourgeat@lcpp.cpe.fr.

Notes

The authors declare no competing financial interest.

■ REFERENCES

(1) Hajji, P.; David, L.; Gerard, J. F.; Pascault, J. P.; Vigier, G. Synthesis, structure, and morphology of polymer-silica hybrid nanocomposites based on hydroxyethyl methacrylate. *J. Polym. Sci., Part B: Polym. Phys.* **1999**, *37*, 3172–3187.

(2) Xiong, M.; Wu, L.; Zhou, S.; You, B. Preparation and characterization of acrylic latex/nano-SiO_2 composites. *Polym. Int.* **2002**, *51*, 693–698.

(3) Chabert, E.; Bornert, M.; Bourgeat-Lami, E.; Cavaillé, J-Y.; Dendievel, R.; Gauthier, C.; Putaux, J-L.; Zaoui, A. Filler–filler interactions and viscoelastic behavior of polymer nanocomposites. *Mater. Sci. Eng., A* **2004**, *381*, 320–330.

(4) Liu, Y.-L.; Hsu, C.-Y.; Hsu, K.-Y. Poly(methylmethacrylate)-silica nanocomposite films from surface-functionalized silica nanoparticles. *Polymer* **2005**, *46*, 1851–1856.

(5) Amerio, E.; Fabbri, P.; Malucelli, G.; Messori, M.; Sangermano, M.; Taurino, R. Scratch resistance of nano-silica reinforced acrylic coatings. *Prog. Org. Coat.* **2008**, *62*, 129–133.

(6) Zhou, S.; Xiong, M.; Wu, L. the properties of high solid acrylic based polyurethane and acrylic latex embedded with nano-silica. *J. Chem. Eng. Jpn.* **2003**, *36*, 1263–1269.

(7) Daoud, W. A.; Xin, J. H.; Tao, X. Synthesis and characterization of hydrophobic silica nanocomposites. *Appl. Surf. Sci.* **2006**, *252*, 5368–5371.

(8) Zou, H.; Wu, S.; Shen, J. Polymer/silica nanocomposites: preparation, characterization, properties, and applications. *Chem. Rev.* **2008**, *108*, 3893–3957.

(9) Bourgeat-Lami, E.; Lansalot, M. Organic/inorganic composite latexes: the marriage of emulsion polymerization and inorganic chemistry. *Adv. Polym. Sci.* **2010**, *233*, 53–123.

(10) Luna-Xavier, J-L.; Guyot, A.; Bourgeat-Lami, E. Preparation of nano-sized silica/poly(methyl methacrylate) composite latexes by heterocoagulation: comparison of three synthetic routes. *Polym. Int.* **2004**, *53*, 609–617.

(11) Zeng, Z.; Yu, J.; Guo, Z. X. Preparation of polymer/silica composite nanoparticles bearing carboxyl groups on the surface via emulsifier-free emulsion copolymerization. *J. Polym. Sci., Part A: Polym. Chem.* **2005**, *43*, 2826–2835.

(12) Negrete-Herrera, N.; Putaux, J-L.; David, L.; Bourgeat-Lami, E. Polymer/laponite composite colloids through emulsion polymerization: influence of the clay modification level on particle morphology. *Macromolecules* **2006**, *39*, 9177–9184.

(13) Bourgeat-Lami, E.; Insulaire, M.; Reculusa, S.; Perro, A.; Ravaine, S.; Duguet, E. Nucleation of polystyrene latex particles in the presence of γ-methacryloxypropyl trimethoxysilane-functionalized silica particles. *J. Nanosci. Nanotechnol.* **2006**, *6*, 432–444.

(14) Weiss, C. K.; Landfester, K. Miniemulsion polymerization as a means to encapsulate organic and inorganic materials. *Adv. Polym. Sci.* **2010**, *233*, 185–236.

(15) Hu, J.; Chen, M.; Wu, L. Organic-inorganic nanocomposites synthesized via miniemulsion polymerization. *Polym. Chem.* **2011**, *2*, 760–772.

(16) Forcada, J.; Ramos, J. Encapsulation of Inorganic Nanoparticles by Miniemulsion Polymerization. In *Miniemulsion Polymerization Technology*; Mittal, V., Ed.; John Wiley & Sons: Hoboken, NJ, 2010; Chapter 4,.

(17) Tiarks, F.; Landfester, K.; Antonietti, M. Silica nanoparticles as surfactants and fillers for latexes made by miniemulsion polymerization. *Langmuir* **2001**, *17*, 5775–5780.

(18) Zhang, S.; Zhou, S.; Weng, Y.; Wu, L. Synthesis of SiO_2/polystyrene nanocomposite particles via miniemulsion polymerization. *Langmuir* **2005**, *21*, 2124−2128.
(19) Zhou, J.; Zhang, S.; Qiao, X.; Li, X.; Wu, L. Synthesis of SiO_2/poly(styrene-co-butyl acrylate) nanocomposite microspheres via miniemulsion polymerization. *J. Polym. Sci., Part A: Polym. Chem.* **2006**, *44*, 3202−3209.
(20) Qi, D.-M.; Bao, Y.-Z.; Weng, Z.-X.; Huang, Z.-M. Preparation of acrylate polymer/silica nanocomposite particles with high silica encapsulation efficiency via miniemulsion polymerization. *Polymer* **2006**, *47*, 4622−4629.
(21) Costoyas, A.; Ramos, J.; Forcada, J. Encapsulation of silica nanoparticles by miniemulsion polymerization. *J. Polym. Sci., Part A: Polym. Chem.* **2009**, *47*, 935−948.
(22) Qiao, X.; Chen, M.; Zhou, J.; Wu, L. Synthesis of raspberry-like silica/polystyrene/silica multilayer hybrid particles via miniemulsion polymerization. *J. Polym. Sci., Part A: Polym. Chem.* **2007**, *45*, 1028−1037.
(23) Zhang, Y.; Chen, H.; Shu, X.; Zou, Q.; Chen, M. Fabrication and characterization of raspberry-like PSt/SiO_2 composite microspheres via miniemulsion polymerization. *Colloids Surf., A* **2009**, *350*, 26−32.
(24) Qiang, W.; Wang, Y.; He, P.; Xu, H.; Gu, H.; Shi, D. Synthesis of asymmetric inorganic/polymer nanocomposite particles via localized substrate surface modification and miniemulsion polymerization. *Langmuir* **2008**, *24*, 606−608.
(25) Liu, B.; Zhang, C.; Liu, J.; Qu, X.; Yang, Z. Janus non-spherical colloids by asymmetric wet-etching. *Chem. Commun.* **2009**, 3871−3873.
(26) Yin, Y.; Zhou, S.; You, B.; Wu, L. Facile fabrication and self-assembly of polystyrene−silica asymmetric colloid spheres. *J. Polym. Sci., Part A: Polym. Chem.* **2011**, *49*, 3272−3279.
(27) Lu, W.; Chen, M.; Wu, L. One-step synthesis of organic-inorganic hybrid asymmetric dimer particles via miniemulsion polymerization and functionalization with silver. *J. Colloid Interface Sci.* **2008**, *328*, 98−102.
(28) (a) Bailly, B.; Donnenwirth, A. C.; Bartholome, C.; Beyou, E.; Bourgeat-Lami, E. Silica-polystyrene nanocomposite particles synthesized by nitroxide-mediated polymerization and their encapsulation through miniemulsion polymerization. *J. Nanomater.* **2006**, *2006*, 1−10. (b) Konn, C.; Morel, F.; Beyou, E.; Chaumont, P.; Bourgeat-Lami, E. Nitroxide-mediated polymerization of styrene initiated from the surface of laponite clay platelets. *Macromolecules* **2006**, *40*, 7464−7472.
(29) Bombalski, L.; Min, K.; Dong, H.; Tang, C.; Matyjaszewski, K. Preparation of well-defined hybrid materials by ATRP in miniemulsion. *Macromolecules* **2007**, *40*, 7429−7432.
(30) Töpfer, O.; Schmidt-Haake, G. Surface-functionalized inorganic nanoparticles in miniemulsion polymerization. *Macromol. Symp.* **2007**, *248*, 239−248.
(31) Lu, S.; Forcada, J. Preparation and characterization of magnetite polymeric composite particles by miniemulsion polymerization. *J. Polym. Sci., Part A: Polym. Chem.* **2006**, *44*, 4187−4203.
(32) Kim, H.; Daniels, E. S.; Li, S.; Mokkapati, V. K.; Kardos, K. Polymer encapsulation of yttrium oxysulfide phosphorescent particles via miniemulsion polymerization. *J. Polym. Sci., Part A: Polym. Chem.* **2007**, *45*, 1038−1054.
(33) Diaconu, G.; Paulis, M.; Leiza, J. R. High solids content waterborne acrylic/ montmorillonite nanocomposites by miniemulsion polymerization. *Macromol. React. Eng.* **2008**, *2*, 80−89.
(34) van Berkel, K. Y.; Piekarski, A. M.; Kierstead, P. H.; Pressly, E. D.; Ray, P. C.; Hawker, C. J. A simple route to multimodal composite nanoparticles. *Macromolecules* **2009**, *42*, 1425−1427.
(35) Erdem, B.; Sudol, E. D.; Dimonie, V. L.; El-Aasser, M. S. Encapsulation of inorganic particles via miniemulsion polymerization. I. Dispersion of titanium dioxide particles in organic media using OLOA 370 as stabilizer. *J. Polym. Sci., Part A: Polym. Chem.* **2000**, *38*, 4419−4430.
(36) Bourgeat-Lami, E.; Lang, J. Encapsulation of inorganic particles by dispersion polymerization in polar media: 1. Silica nanoparticles encapsulated by polystyrene. *J. Colloid Interface Sci.* **1998**, *197*, 293−308.
(37) Sunkara, H. B.; Jethmalani, J. M.; Ford, W. T. Composite of colloidal crystals of silica in poly(methyl methacrylate). *Chem. Mater.* **1994**, *6*, 362−364.
(38) Jethmalani, J. M.; Ford, W. T. Diffraction of visible light by ordered monodisperse silica-poly(methyl acrylate) composite films. *Chem. Mater.* **1996**, *8*, 2138−2146.
(39) Hiltner, P. A.; Papir, Y. S.; Krieger, I. M. Diffraction of light by non-aqueous ordered suspensions. *J. Phys. Chem.* **1971**, *75*, 1881−1886.
(40) Brunauer, S.; Emmett, P. H.; Teller, E. Adsorption of gases in multimolecular layers. *J. Am. Chem. Soc.* **1938**, *60*, 309−319.
(41) (a) Koppel, D. E. Analysis of macromolecular polydispersity in intensity correlation spectroscopy: the method of cumulants. *J. Chem. Phys.* **1972**, *57*, 4814−4820. (b) *Methods for Determination of Particle Size Distribution*; International Standard ISO 13321; International Organization for Standardization (ISO): Geneva, 1996; Part 8.
(42) Lin, M.; Chu, F.; Guyot, A.; Putaux, J.-L.; Bourgeat-Lami, E. Silicone-polyacrylate composite latex particles. Particles formation and film properties. *Polymer* **2005**, *46*, 1331−1337.
(43) (a) Philipse, A. P.; Vrij, A. Preparation and properties of nonaqueous model dispersions of chemically modified, charged silica spheres. *J. Colloid Interface Sci.* **1989**, *128*, 121−136. (b) Philipse, A. P.; Vrij, A. Solid opaline packings of colloidal silica spheres. *J. Mater. Sci. Lett.* **1989**, *8*, 1371−1373.
(44) Plueddeman, E. P. *Silane coupling agent*; Plenum Press: New York, 1991.
(45) Posthumus, W.; Magusin, P. C. M. M.; Brokken-Zijp, J. C. M.; Tinnemans, A. H. A.; van der Linde, R. Surface modification of oxidic nanoparticles using 3-methacryloxypropyl trimethoxysilane. *J. Colloid Interface Sci.* **2004**, *269*, 109−116.
(46) Liu, X.; Zhao, H.; Li, L.; Yan, J.; Zha, L. Preparation of silica/poly(tert-butylmethacrylate) core/shell nanocomposite latex particles. *J. Macromol. Sci., Part A: Pure Appl. Chem.* **2006**, *43*, 1757−1764.
(47) Berendsen, G. E.; Galan, L. D. Preparation and chromatographic properties of some chemically bonded phases for reversed-phase liquid chromatography. *J. Liq. Chromatogr.* **1978**, *1*, 561−586.
(48) Iijima, M.; Tsukada, M.; Kamiya, H. Effect of particle size on surface modification of silica nanoparticles by using silane coupling agents and their dispersion stability in methylethylketone. *J. Colloid Interface Sci.* **2007**, *307*, 418−424.
(49) Deng, Y. H.; Wang, C. C.; Hu, J. H.; Yang, W. L.; Fu, S. K. Investigation of formation of silica-coated magnetite nanoparticles via sol−gel approach. *Colloids Surf., A* **2005**, *262*, 87−93.
(50) Guinier, A.; Fournet, G. *Small-Angle Scattering of X-rays*; John Wiley & Sons: New York, 1955.
(51) Pearson, K. Mathematical contributions to the theory of evolution. XIX. Second supplement to a memoir on skew variation. *Philos. Trans. R. Soc. London, Ser. A* **1916**, *216*, 429−457.
(52) Kotlarchyk, M.; Stephens, R. B.; Huang, J. S. Study of Schultz distribution to model polydispersity of microemulsion droplets. *J. Phys. Chem.* **1988**, *92*, 1533−1538.
(53) Erdem, B.; Sudol, E. D.; Dimonie, V. L.; El-Aasser, M. S. Encapsulation of inorganic particles viaminiemulsion polymerization (II). Preparation and characterization of styrene miniemulsion droplets containing TiO_2 particles. *J. Polym. Sci., Part A: Polym. Chem.* **2000**, *38*, 4431−4440.
(54) Erdem, B.; Sudol, E. D.; Dimonie, V. L.; El-Aasser, M. S. Encapsulation of inorganic particles via miniemulsion polymerization. III. Characterization of encapsulation. *J. Polym. Sci., Part A: Polym. Chem.* **2000**, *38*, 4441−4450.
(55) Binks, B. P.; Lumsdon, S. O. Pickering emulsions stabilized by monodisperse latex particles: effects of particle size. *Langmuir* **2001**, *17*, 4540−4547.
(56) Frelichowska, J.; Bolzinger, M. A.; Chevalier, Y. Effects of solid particle content on properties of o/w Pickering emulsions. *J. Colloid Interface Sci.* **2010**, *351*, 348−356.

(57) Mabille, C.; Leal-Calderon, F.; Bibette, J.; Schmitt, V. Monodisperse fragmentation in emulsions: mechanisms and kinetics. *Europhys. Lett.* **2003**, *61*, 708−714.
(58) (a) Hansen, F. K.; Ugelstad, J. Nucleation in monomer droplets. *J Polym. Sci., Polym. Lett. Ed.* **1979**, *17*, 3069−3082. (b) Azad, A. R. M.; Ugelstad, J.; Fitch, R. M.; Hansen, F. K. In *Emulsion Polymerization*; ACS Symposium Series 24; Piirma, I., Gardon, J. L., Eds.; American Chemical Society: Washington, DC, 1976; p 1.
(59) Choi, Y. T. Formation and Stabilization of Miniemulsions and Latexes. Ph.D. Dissertation, Lehigh University, 1985.
(60) Vignati, E.; Piazza, R.; Lockart, T. Pickering emulsions: interfacial tension, colloidal layer morphology, and trapped-particle motion. *Langmuir* **2003**, *19*, 6650−6656.
(61) Fitch, R. M.; Tsai, C. H. Polymer colloids: Particle formation in non micellar systems. *J. Polym. Sci., Part B: Polym. Lett.* **1970**, *8*, 703−710.
(62) Bourgeat-Lami, E.; Espiard, P.; Guyot, A.; Gauthier, C.; David, L.; Vigier, G. Emulsion polymerization in the presence of colloidal silica particles: application of the reinforcement of poly(ethyl acrylate) films. *Angew. Makromol. Chem.* **1996**, *242*, 105−122.